

Article

Degradable Magnesium and Its Surface Modification as Tumor Embolic Agent for Transcatheter Arterial Chemoembolization

Xinbao Kang ¹, Yonggang Wang ², Hongtao Li ², Han Yu ¹, Xiyue Zhang ¹, Rui Zan ^{3,4}, Wenhui Wang ^{1,*}, Tao Wang ^{5,*} and Xiaonong Zhang ^{1,4,6,*}

¹ State Key Laboratory of Metal Matrix Composites, School of Materials Science and Engineering, Shanghai Jiao Tong University, Shanghai 200240, China

² Department of Oncology, Shanghai Jiao Tong University Affiliated Sixth People's Hospital, Shanghai 200233, China

³ Department of General Surgery, Zhongshan Hospital, Fudan University, Shanghai 200032, China

⁴ Shanghai Engineering Research Center of Biliary Tract Minimal Invasive Surgery and Materials, Shanghai 200032, China

⁵ Department of Emergency Trauma Center, Tongji Hospital, Tongji University School of Medicine, Shanghai 200065, China

⁶ Suzhou Origin Medical Technology Co., Ltd., Suzhou 215513, China

* Correspondence: wenhuiwang@sjtu.edu.cn (W.W.); happywt0403@sina.com (T.W.); xnzhang@sjtu.edu.cn (X.Z.)

Abstract: Transcatheter arterial chemoembolization (TACE) is an effective method for traditional cancer treatment. Currently, various embolic agents block the blood vessels in the TACE operation. In this paper, the feasibility of the degradable Mg applied for TACE was explored innovatively. The degradation behavior of Mg particles and PLLA modified Mg particles used as embolic agents in contrast media was studied. The morphology and corrosion products were also characterized. After two days of immersion, the pH of the contrast agent was increased to 9.79 and 10.28 by the PLLA-modified Mg particles and unmodified Mg, respectively. The results show that the surface-modified Mg particles with PLLA have an eligible degradation rate to release degradation products and form an acceptable microenvironment. It is feasible to be used as an embolic agent in TACE.

Keywords: magnesium; biodegradable; PLLA; transcatheter arterial chemoembolization; corrosion



Citation: Kang, X.; Wang, Y.; Li, H.; Yu, H.; Zhang, X.; Zan, R.; Wang, W.; Wang, T.; Zhang, X. Degradable Magnesium and Its Surface Modification as Tumor Embolic Agent for Transcatheter Arterial Chemoembolization. *Crystals* **2023**, *13*, 194. <https://doi.org/10.3390/cryst13020194>

Academic Editors: Mădălina Simona Bălțatu, Andrei Victor Sandu and Petrica Vizureanu

Received: 19 December 2022

Revised: 15 January 2023

Accepted: 17 January 2023

Published: 22 January 2023



Copyright: © 2023 by the authors. Licensee MDPI, Basel, Switzerland. This article is an open access article distributed under the terms and conditions of the Creative Commons Attribution (CC BY) license (<https://creativecommons.org/licenses/by/4.0/>).

1. Introduction

As the second common disease worldwide, the incidence rate and mortality of cancer have continued to increase in the last ten years. According to the international agency's report for cancer research, there were 18.1 million new cancer patients and 9.6 million deaths in 2018 [1]. The global cancer statistics in 2020 show 19.3 million new cancer cases and nearly 10 million deaths [2]. In short, cancer's threat to human life and health can still not be underestimated. In order to overcome the problems in traditional treatment, many scholars have explored new treatments, and TACE is one of them. TACE eliminates tumors through the simultaneous action of chemotherapeutic drugs and embolic agents. In the treatment of liver cancer, TACE is primarily used for patients with medium-term liver cancer, particularly those unable to receive surgical treatment [3].

TACE can be divided into four types: convention TACE (c-TACE) [4], balloon occlusion TACE [4], drug-eluting bead TACE (DEB-TACE) [5] and trans arterial radioembolization (TARE) [5]. The four TACE methods have their advantages and disadvantages, and the treatment scheme needs to be considered in combination with the actual situation of patients. On one hand, the appropriate drugs should be selected to cooperate with embolic agents. On the other hand, the side effects caused by the early release of drugs should be avoided as much as possible.

Mg has important research and application value in basic science [6,7], industrial energy [8] and other fields, among which biodegradable Mg is one of the most popular biomedical metal materials to date. The research of biomedical Mg alloys can be traced back to the 1870s. In 1878, Edward C. Huse inserted a Mg wire into a patient's body as a hemostatic bandage, found that the degradation rate of it in human body was slow, and proved that the time required for the complete degradation of the Mg wire was related to its diameter [9]. After that, Mg and its alloys began to receive the attention of the relevant scholars. At the end of the 19th century, Payr put forward the idea of using Mg in surgery and put it into practice. In 1900, when he used a Mg tube as a connector to anastomose blood vessels, he found that placing the tube inside the blood vessel would cause blood coagulation and, in severe cases, would cause thrombus [10]. Using the coagulation effect of Mg, he tried to use it for the treatment of hemangioma and found that the Mg alloy can transform early hemangioma into fibrous tissue [11,12]. In addition, he has also conducted research on the use of Mg plates to suture human liver and spleen [10,13]. His work has greatly promoted the application of Mg in medical fields. Subsequently, an increasing number of scholars began to research Mg and its alloys as biomedical materials [14].

In 1907, Lambotte used a Mg plate and screw in the treatment of humeral fracture in children. The patients recovered well after the operation, and no infection or other adverse reactions were observed in the surrounding tissues [14,15]. Subsequently, Verbrugge et al. also used Mg-based bone nails and plates in the treatment of humeral fractures. Three weeks after operation, the implants had been completely degraded in the patient [16–18]. In 1940, Maier treated humeral fractures with a bone pin made of Mg. In the following 14 years, the patients recovered well without any side effects caused by the treatment [19]. In the middle of the 20th century, Trotskii and Tsitrin used Mg-Cd alloy plates and screws to treat pseudoarthrosis and found that new cortical bone was formed around the Mg alloy implant. The implant itself completely degraded [20].

Although the relevant research on Mg as a biomedical material continues, the degradation rate of magnesium and its alloys cannot be reduced to the expected level, and the corrosion mechanism of magnesium is still unclear, leading to the problem that the mechanical properties of magnesium and its alloys cannot be maintained for a long time. At the same time, stainless steel and titanium (Ti) alloys are increasingly used in the biomedical field, while Mg and its alloys are less frequently researched in the medical field. However, with the further development of corrosion science and the progress of material processing technology, researchers have been able to control the degradation rate of Mg and its alloys by a variety of means, which has brought biomedical Mg alloys back into view in medical research.

Although Mg and its alloys have been extensively studied in the biomedical field, no researchers have tried to use Mg as an embolic agent in the TACE process. Mg is an essential element for the human body and has been the subject of great interest in clinical research as a biodegradable implantation due to its superior biodegradability and biocompatibility [21]. Under a physiological environment, Mg will degrade spontaneously to Mg^{2+} through the electrochemical corrosion process and reduce its H_2O to H_2 , increasing the local pH [22]. The research results of Bois et al. showed that rats lacking Mg had a higher probability of thymic lymphoid carcinoma, which increased with the prolongation of Mg deficiency [23]. Some studies have also pointed out that $Mg(OH)_2$ has a preventive effect on colorectal cancer in rats. Tanaka et al. found that colorectal cancer in rats, induced by carcinogens, can be inhibited by $Mg(OH)_2$, and the inhibitory effect of low-dose $Mg(OH)_2$ is more substantial [24]. Our recent work also indicates that the degradation products Mg^{2+} and H_2 can restrain the activity of tumor cells and decrease reactive oxygen species (ROS) [25]. Therefore, a Mg-modified embolic agent seems to be a feasible way to improve the anticancer effect of TACE, which is worth exploring (Figure 1).

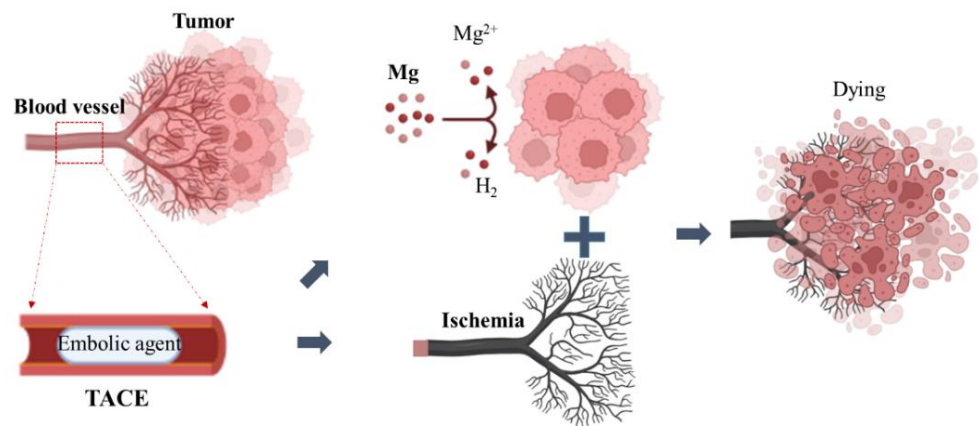


Figure 1. Effect of degradable Mg particles as embolic agents in TACE. The degradation products of Mg can inhibit tumor, and the embolization of particles can block tumor blood supply.

According to the Pilling-Bedworth principle, Mg cannot form a dense oxide film to prevent its further oxidation during the oxidation process [26]. Therefore, to control the degradation rate of Mg requires surface modification. A large number of studies have shown that surface modification technology will not only effectively slow down the degradation rate of Mg alloys [27,28], but give them special biological functions [29,30]. It is the most widely used technology to improve their degradation performance in vivo.

Mousa et al. prepared a layer of ceramic coating containing Zr by electrodeposition and found that the coating can improve the corrosion resistance and biocompatibility of the Mg alloy [29]. Gu et al. obtained a dense Mg oxide coating after alkali heat treatment on the surface of the Mg alloy and proved that this coating can effectively improve the corrosion resistance and biocompatibility of the Mg alloy [30]. Xu et al. successively proved the protective effect of a micro-arc oxidation coating on Mg by measuring the weight loss and hydrogen evolution of Mg after micro-arc oxidation in the corrosion process [31]. Zhao et al. proved through in vivo and in vitro experiments that a chitosan coating will not only reduce the degradation rate of the Mg alloy orthopedic implants, but also improve its biocompatibility [32].

In the process of using Mg as an embolic agent in TACE, selecting the appropriate coating materials can enhance its therapeutic effect. PLLA is cheap and has good biocompatibility and biodegradability. As a result, it has been used in many practical medical devices and is a reasonably mature coating material. However, due to the weak binding force between magnesium and PLLA, it is prone to falling off during use; therefore, PLLA is not generally used alone to modify. Zeng et al. prepared a MAO/PLLA composite coating on the surface of a magnesium alloy by micro-arc oxidation technology and found that this coating can significantly improve the corrosion resistance of the magnesium alloy [33].

As an embolic material, the Mg particles are injected into tumor blood vessels through microcatheters to block the blood vessels and cause tumor necrosis. In order to introduce Mg particles into the tumor blood vessels, they must be mixed with a medical contrast agent so that the position of the implanted Mg particles can be observed in real-time by angiography to ensure that they can accurately reach the tumor. In this work, we produced Mg particles and mixed the particles with the contrast agent to explore the degradation of the Mg in the contrast agent. The results showed that the unmodified Mg degraded too quickly in the contrast medium and would destroy the practical structure of the contrast medium; the PLLA modified Mg can overcome these two problems. This work is the first to explore Mg's feasibility as a tumor embolic agent. It will provide an innovative idea for the TACE treatment of tumors, and bring a novel expansion for the clinical application of biodegradable Mg.

2. Materials and Methods

2.1. Materials

Suzhou Origin Medical Technology Co. Ltd., China, provided the as-casted ingots of Mg with a high purity of 99.98% selected for this research. The chemical compositions of the high-purity Mg (HPM) were analyzed using a plasma-atomic emission spectrometer (ICP-AES), and the results are listed in Table 1 [34].

Table 1. Chemical compositions of HPM as analyzed by ICP-AES. Reprinted with permission from Ref. [34]. 2020, Elsevier.

Element	Mg	Si	Fe	Ni	Cu	Al	Mn	Ti	Pb	Sn	Zn
ppmw	Bal.	20	20	5	5	20	20	10	10	5	20

First, the HPM ingot was hot-extruded, and the extrusion temperature was 350 °C. The Mg ingot with a diameter of 20 mm was extruded and thinned to about 1 mm. Then, three passes of hot drawing were carried out, and the preset temperatures were 190 °C, 170 °C, and 130 °C, respectively. Finally, Mg wires with a diameter of 0.25 mm was obtained. They were cut into cylindrical Mg particles with a length of 0.50 mm.

In this experiment, the contrast agent with ioversol ($C_{18}H_{24}I_3N_3O_9$) as the main component was used as the corrosion solution. Other components included aminobutanol ($C_4H_{11}NO_3$), calcium sodium edetate ($C_{10}H_{12}CaN_2Na_2O_8$), and water. The pH was approximately 7 (6.87–7.04), as measured by a pH meter (Mettler Toledo Fe20).

2.2. Microstructure

The drawn HPM wire was hot-mounted with a metallographic inlay machine (XQ-2B), and then the samples were polished with 240-mesh, 800-mesh, 1200-mesh, and 4000-mesh sandpaper in turn. Afterward, the samples were polished on a polishing cloth using a W1 diamond paste. Anhydrous ethanol was continuously added, dropwise, during the polishing process to prevent the sample's surface being oxidized.

The metallographic etchant of the sample was prepared, and the composition is shown in Table 2. we used absorbent cotton balls dipped in an etchant to gently wipe the sample's surface, washed with absolute ethanol after etching for 10 s, and dried at room temperature. We observed the sample under a metallographic microscope (CMM-500) and photographed its microstructure.

Table 2. Chemical composition of HPM metallographic etchant.

Composition	Nitric Acid	Acetic Acid	Oxalic Acid	Water
Content	1 mL	1 mL	1 g	150 mL

2.3. Surface Modification

A small amount of CH_2Cl_2 and 3 g 15 w molecular of left-handed polylactic acid (PLLA) were added into a glass bottle; the bottle was sealed and heated in a water bath until all of the PLLA dissolved. A CH_2Cl_2 solution of PLLA was mixed with 0.6 g Mg particles; this mixture was then fully vibrated to cause the Mg particles to disperse evenly in the solution, then the glass bottle was placed in a water bath to heat, and taken out after 1 h. The Mg particles in the glass bottle were transferred to the empty bottle and dried under a vacuum environment at room temperature for 24 hours to obtain the Mg particles that were modified by the PLLA coating.

2.4. Corrosion Test

The ratio of embolic agent to contrast agent was 1 g:15 mL to test the corrosion rate of the degradable Mg particles in the contrast agent. First, 0.2 g Mg particles were weighed with an analytical balance (Denver Instrument TP-214) three times and put into three 10 mL

beakers. Then, 3×3 mL of medical contrast agent were drawn with a pipette gun and injected into the three beakers. The beakers were sealed with plastic wrap to prevent the volatilization of the contrast agent. The three beakers were subsequently placed in a dark place. The corrosion rate of the degradable Mg particles in the contrast medium was characterized by measuring the change in pH of the contrast medium with immersion time. A small amount of Mg particles was taken out from the beaker at a particular time. After drying, the corrosion morphology was photographed by the scanning electron microscope with EDS (SEM, Rise). Two groups of samples soaked in the contrast medium were selected for testing.

3. Results and Discussion

Figure 2a demonstrates the microstructure of the Mg wire before being cut into particles. The grain is relatively homogeneous, with an average size of $16 \mu\text{m}$, as measured by the line cut method (Figure 2b). Figure 2c shows that the pH of the contrast medium changes with the immersion time of the Mg particles and the PLLA modified Mg particles. It can be seen that the corrosion rate of the Mg particles after PLLA coating has been better controlled. Compared with the Mg group, with a pH of 7.99 after soaking for 10 min, the pH of the group with the PLLA coating remains below 7.86 after soaking for 40 min. After soaking for two days, the pH of the contrast medium of the PLLA modified Mg particles is 9.79, while the pH of the contrast medium of modified Mg particles is 10.28, which further proves that the PLLA coating can slow down the corrosion rate of the Mg particles in the contrast medium, at least within 48 h.

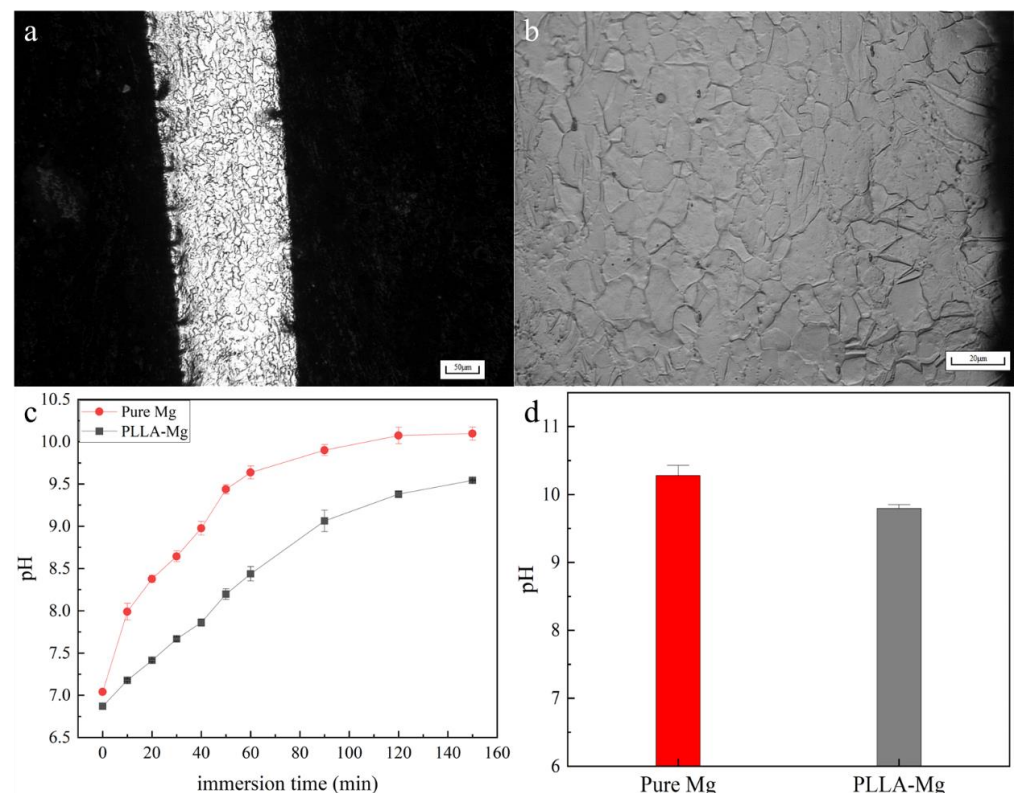


Figure 2. Metallography and the evolution of pH. (a,b) Microstructure of Mg wire before cutting into particles. (c) The pH of the contrast medium changes with the immersion time (0–150 min) of the Mg particles and the PLLA modified Mg particles. (d) The pH of the contrast medium after 2 days immersion of Mg particles and PLLA modified Mg particles.

According to the research of Lou et al. [35], after soaking high-purity Mg tablets in PBS for 24 h, the pH of the solution did not exceed 7.8. After soaking for seven days, the

pH of the solution remained stable, between 8.2–8.3, which is far less than the pH rise rate measured in this study. On one hand, this is related to the larger specific surface area of the Mg particles. On the other hand, the corrosivity of the contrast media also deserves attention.

Figure 3 demonstrates the corrosion morphology of the Mg particles soaked in a contrast medium for 0, 1 h, 2 h, 2 d and 30 d at 300× and 1000× magnification, respectively. It can be seen that the micromorphology of the Mg particles is flat but not smooth. The surface of the Mg particles soaked in a contrast medium for 1 h and 2 h has a relatively smooth corrosion film, with cracks, which should be chapped by dehydration. This shell layer is the corrosion product formed in the initial stage of the corrosion reaction. The Mg particles soaked in a contrast medium for 2 d and 30 d can still observe this shell layer, but the shell is no longer flat and full of cracks and small fragments. This phenomenon indicates that the corrosion reaction has entered another stage, and the generated flat corrosion product shell has also been attacked.

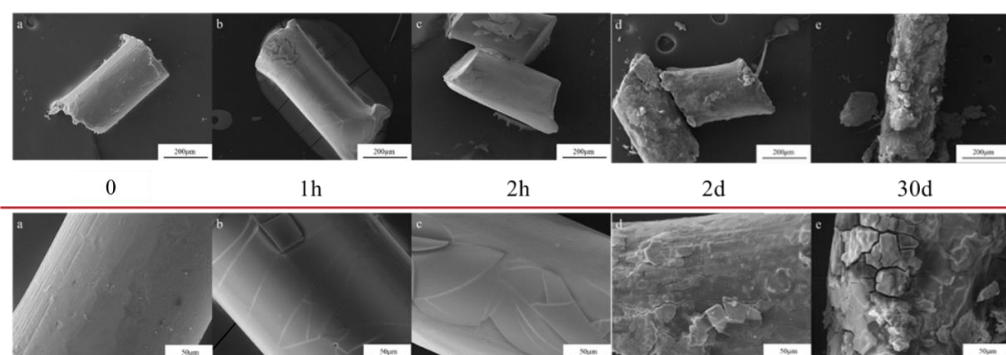


Figure 3. Micro morphology of Pure-Mg particles after corrosion under different magnification.

The primary corrosion film of Mg in the physiological environment is $\text{Mg}(\text{OH})_2$, which can prevent the dissolution of anode Mg and the H_2 evolution reaction of the cathode and has a protective effect. According to previous literature reports, a $\text{Mg}(\text{OH})_2$ film will decompose in the presence of Cl^- , thus greatly reducing its protection. Comparing the experimental results of Zuo, it can be found that the corrosion rate of pure Mg in the contrast agent is much higher than that in m-SBF, artificial urine, and bile [36]. Moreover, these solutions do not contain the I element. Therefore, it can be considered that the Mg has a higher corrosion rate in ioversol, and then I^- may have a destructive effect on $\text{Mg}(\text{OH})_2$, such as Cl^- .

Figure 4 shows the corrosion morphology of the Mg particles with PLLA modification soaked in the contrast medium for 0, 1 h, 2 h, 3 h, 4 h and 2 d at 300× and 1000× magnification, respectively. There is an irregular shell on the surface of the modified magnesium particles, which is a PLLA coating. After soaking for 1 h, the PLLA shell has disappeared but, at this time, the surface of the Mg particles is not completely covered by the corrosion products. The flat shell, which was also seen in the previous section, appeared on the surface of the Mg particles soaked for 2 h, and the detached PLLA has adhered to the shell. The difference in the corrosion morphology can be seen at 2 h. The $\text{Mg}(\text{OH})_2$ film with cracks can be observed on the surface of the pure Mg group, but no cracking of the film is found on the surface of the PLLA-modified group. After two days of immersion, a lot of the degradation products precipitated in the pure Mg group, while the PLLA group was relatively smooth without a large amount of product accumulation. After that, with the extension of the soaking time, only the cracking of the shell of the corrosion products increased, but the fragmented corrosion products in Figure 3 could not be observed. These results indicate that PLLA can effectively protect the magnesium matrix in contrast media. However, it is found that the corrosion rate of the Mg particles modified by PLLA in the contrast agent is still higher than that of the pure Mg in the PBS solutions [36], indicating

that the chemical composition of the contrast agent is aggressivity. The protective effect of PLLA on the magnesium particles is lost due to the corrosion of the contrast agent.

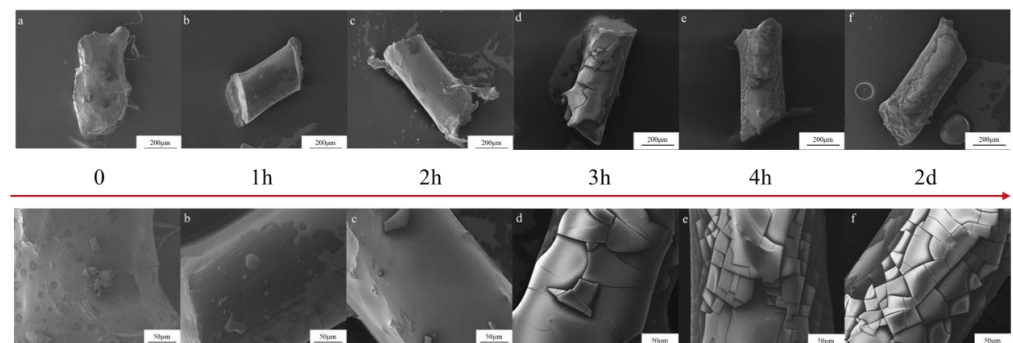


Figure 4. Micro morphology of PLLA-Mg particles after corrosion under different magnifications.

The cross-sectional SEM pictures of the PLLA-modified Mg particles were taken before and after soaking for two days, as shown in Figure 5. The difference between the PLLA coating and the Mg corrosion products can be seen. It can be found that the PLLA coating has poor bonding with the Mg particles, and part of the coating does not adhere to the surface of the particles, while the corrosion products of Mg are well bonded to the matrix, with almost no visible boundaries. From the picture, we can measure that the thickness of the PLLA coating is approximately 5 μm , and that of the corrosion product layer is approximately 4 μm .

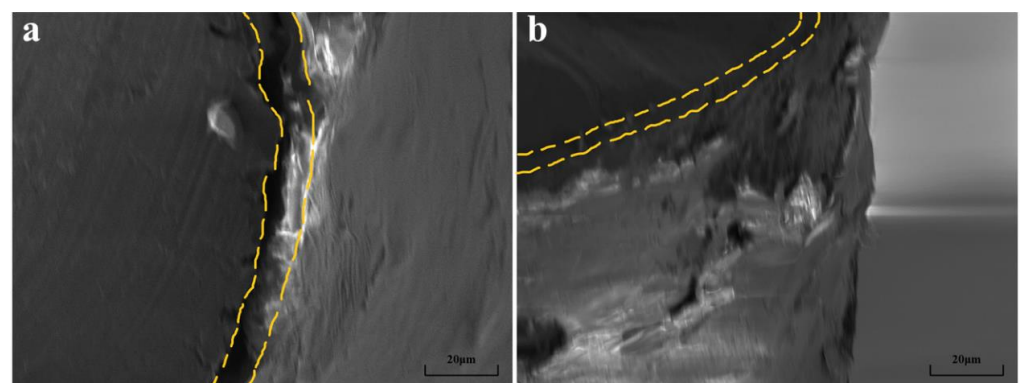


Figure 5. The cross-sectional SEM pictures of the PLLA-modified Mg particles before (a) and after soaking for two days (b).

It is shown in Figure 6a that the corrosion products of the Mg particles mostly contain element C, followed by O, and then Mg, I and Cl. The reaction products in the second stage of corrosion contain significantly more O and I, indicating that the reason for the cracking and corrosion of the smooth corrosion product shell generated in the first stage is that these two elements, particularly I, are involved in the corrosion reaction. As shown in Figure 6b, the atomic percentage of element C in the corrosion product is the largest, followed by O, N and I. After two days of corrosion, the atomic percentage of the elements in the product is not significantly different from that of after one hour, which is different from the corrosion of the unmodified Mg particles. This result indicates that the reaction mechanism between the contrast agent and Mg particles may change after introducing the PLLA coating. The difference of element N in Figure 6b comes from the aminobutyric alcohol in the contrast agent. The Mg particles modified by PLLA will release lactic acid during the corrosion process. The combination of lactic acid and aminobutyric alcohol will increase the content of N on the surface of the particles.

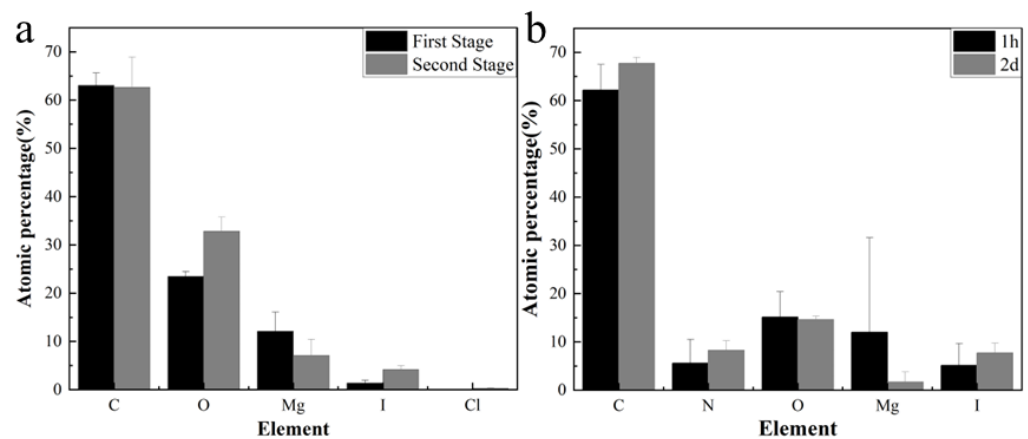


Figure 6. (a) Comparison of atomic percentages of C, O, Mg, I and Cl in point scanning at the first and second stages after two days of Mg particle corrosion. (b) Comparison of atomic percentages of C, N, O, Mg and I in point scanning at 1 h and 2 day of PLLA modified Mg particle corrosion.

The degradation behavior of Mg and PLLA-modified Mg in the contrast agent indicates that the corrosion mechanism in the contrast agent is different from that in simulated body fluid. According to the above reaction, Mg reacts with water in the contrast agent to generate $\text{Mg}(\text{OH})_2$ and first releases H_2 , as shown in Figure 7a. Due to the viscosity of the contrast agent, the generated $\text{Mg}(\text{OH})_2$ will be evenly attached to the surface of the Mg particles to form a passive film. With the progress of corrosion, the water in the contrast medium gradually decreased, and the $\text{Mg}(\text{OH})_2$ shell cracked due to Cl^- attacking. Subsequently, ioversol in the contrast medium decomposes due to light or other conditions and slowly releases I, which exists in the solution as an ion. These released I^- may dissolve the $\text{Mg}(\text{OH})_2$ shell on the surface of the Mg particles and further react to form MgI_2 (Figure 7b). The mechanism at this stage is similar to the dissolution of $\text{Mg}(\text{OH})_2$ by Cl^- .

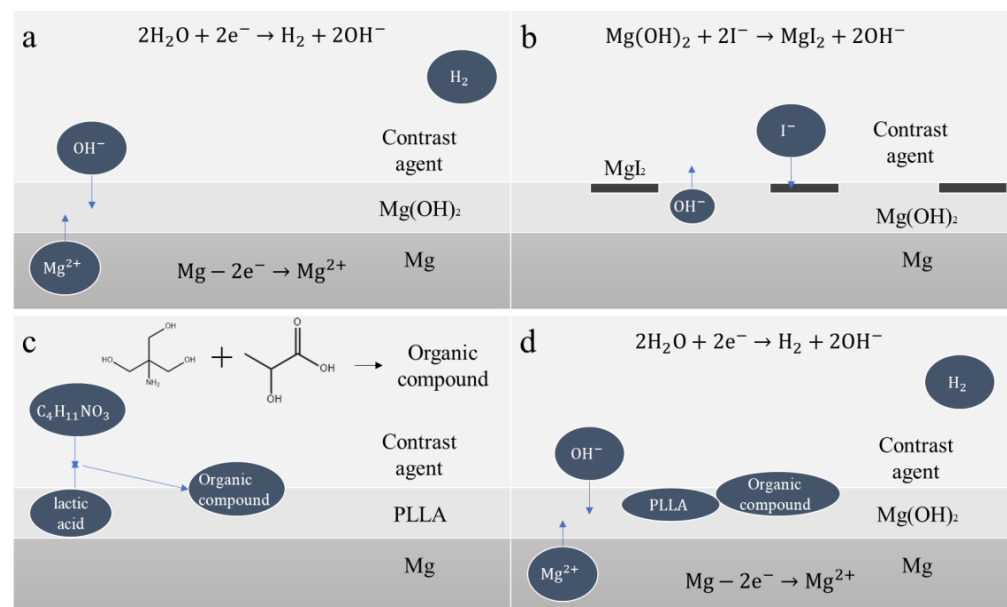


Figure 7. Mechanism of reaction between Mg and contrast agent: pure Mg (a,b) and PLLA modified Mg (c,d).

After surface modification, the PLLA coating on the surface of the Mg particles is corroded by the contrast agent. The generated small molecule lactic acid will combine with amino butanol in the contrast agent and adhere to the surface (Figure 7c). When PLLA is corroded and the Mg surface is exposed to the contrast medium, the corrosion reaction of Mg and water occurs, forming a $\text{Mg}(\text{OH})_2$ shell and releasing H_2 . Subsequently, the corrosion reaction continued. However, as the adsorption process of anion to the Mg matrix is hindered by the PLLA coating, the $\text{Mg}(\text{OH})_2$ film's dissolution by I^- is weakened, and the degradation rate is slowed down (Figure 7d).

In Ref. [36], we obtained the corrosion of HPM in three corrosive media. In this study, we found that the corrosion rate of HPM in ioversol injection is higher than in other corrosive media. In these two articles, we selected HPM provided by the same company, which are consistent in their composition. At the same time, we chose a Mg wire as the experimental material. Although the diameter and length are different, the microstructure is similar. Therefore, we believe that the difference in the corrosion medium is the main reason for the acceleration of the corrosion rate. In the EDS analysis, we found the enrichment of the I element in the corrosion products, while the other three corrosive media did not contain the I element; therefore, we speculate that the I element has an accelerating effect on the corrosion of Mg. Considering that the destructive effect of Cl^- on $\text{Mg}(\text{OH})_2$ has been recognized [37], we suspect that the I element also has the same effect. The difference is that the solubility of MgCl_2 (40 g/100 g) is about five times that of MgI_2 (8.1 g/100 g) at room temperature; thus, the binding ability of I^- is stronger, and the damaging effect on $\text{Mg}(\text{OH})_2$ should also be more apparent.

4. Conclusions

In summary, this work studies the corrosion behavior of pure Mg particles and PLLA-modified Mg particles in an iodofol contrast agent and explores the application of Mg as an embolic agent for TACE. Unmodified pure Mg has a high degradation rate because the contrast agent can decrease the protectiveness of the degradation layer. At the same time, the consumption of I will also lead to a decrease in the effectiveness of the contrast agent itself, which means that a pure Mg is not suitable for TACE. The PLLA-modified Mg can sustain a slow degradation rate within at least 48 h in contrast medium, which effectively reduces the consumption of I and also forms a suitable microenvironment with Mg^{2+} and H_2 release. These findings contribute to broadening the clinical application of biodegradable Mg in the future.

Author Contributions: Data curation, X.K.; Methodology, Y.W.; Supervision, W.W., T.W. and X.Z. (Xiaonong Zhang); Writing—original draft, X.K.; Writing—review and editing, Y.W., H.L., H.Y., X.Z. (Xiyue Zhang) and R.Z. All authors have read and agreed to the published version of the manuscript.

Funding: This research was funded by [National Natural Science Foundation of China] grant number [52201300]; [China Postdoctoral Science Foundation] grant number [2021M702090]; [Changshu Science and Technology Program (Industrial) Project] grant number [CG202107]; [Medical discipline Construction Project of Pudong Health Committee of Shanghai] grant number [2021-03].

Data Availability Statement: Data is unavailable due to privacy restrictions.

Conflicts of Interest: The authors declare no conflict of interest.

References

1. Cucuk, I.A.; Erna, R. Patient's experiences of suffering across the cancer trajectory: A qualitative systematic review protocol. *J. Adv. Nurs.* **2020**, *77*, 1037–1042.
2. Hyuna, S.; Jacques, F. Global Cancer Statistics 2020: GLOBOCAN Estimates of Incidence and Mortality Worldwide for 36 Cancers in 185 Countries. *CA Cancer J. Clin.* **2021**, *71*, 209–249.
3. Boulon, M.; Delhom, E. Transarterial chemoembolization for hepatocellular carcinoma: An old method, now flavor of the day. *Diagn. Interv. Imaging* **2015**, *96*, 607–615. [[CrossRef](#)] [[PubMed](#)]

4. Irie, T.; Kuramochi, M. Dense accumulation of lipiodol emulsion in hepatocellular carcinoma nodule during selective balloon-occluded transarterial chemoembolization: Measurement of balloon-occluded arterial stump pressure. *Cardiovasc. Interv. Radiol.* **2013**, *36*, 706–713. [[CrossRef](#)] [[PubMed](#)]
5. Natthida, K.; Aye, T.N. Yttrium-90 microspheres: A review of its emerging clinical indications. *Liver Cancer* **2015**, *4*, 6–15.
6. Kosar, N.; Gul, S.; Ayub, K.; Bahader, A.; Gilani, M.A.; Arshad, M.; Mahmood, T. Significant nonlinear optical response of alkaline earth metals doped beryllium and magnesium oxide nanocages. *Mater. Chem. Phys.* **2020**, *242*, 122507. [[CrossRef](#)]
7. Kosar, N.; Tahir, H.; Ayub, K.; Gilani, M.A.; Mahmood, T. Theoretical modification of C24 fullerene with single and multiple alkaline earth metal atoms for their potential use as NLO materials. *J. Phys. Chem. Solids* **2021**, *152*, 109972. [[CrossRef](#)]
8. Jia, Y.; Sun, C.H.; Shen, S.H.; Zou, J.; Mao, S.S.; Yao, X.D. Combination of nanosizing and interfacial effect: Future perspective for designing Mg-based nanomaterials for hydrogen storage. *Renew. Sustain. Energy Rev.* **2015**, *44*, 289–303. [[CrossRef](#)]
9. Huse, E.C. A new ligature? *Chic. Med. J. Exam* **1878**, *37*, 171–172.
10. Payr, E. Beiträge zur Technik der Blutgefäß und Nerven-naht nebst Mittheilungen über die Verwendung eines resorbirbaren Metalles in der Chirurgie. *Arch. Klin. Chir.* **1900**, *62*, 67–93.
11. Payr, E. Ueber Verwendung von Magnesium zur Behandlung von Blutgefässerkrankungen. *Dtsch. Z. Für Chir.* **1902**, *63*, 503–511. [[CrossRef](#)]
12. Payr, E. Zur Technik der Behandlung kavernöser Tumoren. *Zent. Chir.* **1903**, *30*, 233–234.
13. Witte, F. The history of biodegradable magnesium implants: A review. *Acta Biomater.* **2010**, *6*, 1680–1692. [[CrossRef](#)] [[PubMed](#)]
14. Zhao, D.; Witte, F.; Lu, F.; Wang, J.; Li, J.; Qin, L. Current status on clinical applications of magnesium-based orthopaedic implants: A review from clinical translational perspective. *Biomaterials* **2017**, *112*, 287–302. [[CrossRef](#)] [[PubMed](#)]
15. Lambotte, A. L'utilisation du magnésium comme matériel perdu dans l'ostéosynthèse. *Bull. Et Mémoires De La Soc. Natl. De Chir.* **1932**, *28*, 1325–1334.
16. Verbrugge, J. La tolérance du tissu osseux vis-à-vis du magnésium métallique. *Presse. Med.* **1933**, *55*, 1112–1114.
17. Verbrugge, J. Le Matériel Métallique Résorbable En Chirurgie Osseuse. *La Presse Med.* **1934**, *23*, 460–465.
18. Verbrugge, J. L'utilisation du magnésium dans le traitement chirurgical des fractures. *Bull. Mem. Soc. Nat. Cir.* **1937**, *59*, 813–823.
19. Maier, O. Über die Verwendbarkeit von Leichtmetallen in der Chirurgie (metallisches Magnesium als Reizmittel zur Knochenneubildung). *Dtsch. Z. Für Chir.* **1940**, *253*, 552–556. [[CrossRef](#)]
20. Troitskii, V.V.; Tsitrin, D.N. The resorbing metallic alloy “Osteosintezit” as material for fastening broken bones. *Khirurgiya* **1944**, *8*, 41–44.
21. Witte, F.; Hort, N. Degradable biomaterials based on magnesium corrosion. *Curr. Opin. Solid State Mater. Sci.* **2009**, *12*, 63–72. [[CrossRef](#)]
22. Bois, P.; Sandborn, E.B. A study of thymic lymphosarcoma developing in magnesium-deficient rats. *Cancer Res.* **1969**, *29*, 763–775. [[PubMed](#)]
23. Wang, W.H.; Carsten, B. A novel lean alloy of biodegradable Mg-2Zn with nanograins. *Bioact. Mater.* **2021**, *6*, 4333–4341. [[CrossRef](#)] [[PubMed](#)]
24. Tanaka, T.; Shinoda, T. Inhibitory effect of magnesium hydroxide on methylazoxymethanol acetate-induced large bowel carcinogenesis in male F344rats. *Carcinogenesis* **1989**, *10*, 613–616. [[CrossRef](#)] [[PubMed](#)]
25. Zan, R.; Ji, W.P. Biodegradable magnesium implants: A potential scaffold for bone tumor patients. *Sci. China Mater.* **2021**, *64*, 1007–1020. [[CrossRef](#)]
26. Liu, Y.; Skedon, P.; Thompson, G.E.; Habazaki, H.; Shimizu, K. Anodic film growth on an Al-21 at.% Mg alloy. *Corros. Sci.* **2002**, *44*, 1133–1142. [[CrossRef](#)]
27. Němcová, A.; Skedon, P.; Thompson, G.E.; Pacal, B. Effect of fluoride on plasma electrolytic oxidation of AZ61 magnesium alloy. *Surf. Coat. Technol.* **2013**, *232*, 827–838. [[CrossRef](#)]
28. Susmita, B.; Samuel, F.R.; Amit, B. Surface modification of biomaterials and biomedical devices using additive manufacturing. *Acta Biomater.* **2018**, *66*, 6–22.
29. Mousa, H.M.; Hussein, K.H.; Woo, H.M.; Park, C.H.; Kim, C.S. One-step anodization deposition of anticorrosive bioceramic compounds on AZ31B magnesium alloy for biomedical application. *Ceram. Int.* **2015**, *41*, 10861–10870. [[CrossRef](#)]
30. Gu, X.N.; Zheng, W.; Cheng, Y.; Zheng, Y.F. A study on alkaline heat treated Mg–Ca alloy for the control of the biocorrosion rate. *Acta Biomater.* **2009**, *5*, 2790–2799. [[CrossRef](#)] [[PubMed](#)]
31. Ma, X.; Zhu, S.; Wang, L.; Ji, C.; Ren, C.; Guan, S. Synthesis and properties of a bio-composite coating formed on magnesium alloy by one-step method of micro-arc oxidation. *J. Alloy. Compd.* **2014**, *590*, 247–253. [[CrossRef](#)]
32. Zhao, J.; Chen, L.; Yu, K.; Chen, C.; Dai, Y.; Qiao, X.; Yan, Y. Biodegradation performance of a chitosan coated magnesium-zinc-tricalcium phosphate composite as an implant. *Bio. Interphases* **2014**, *9*, 031004. [[CrossRef](#)] [[PubMed](#)]
33. Zeng, R.C.; Cui, L.Y.; Jiang, K.; Liu, R.; Zhao, B.D.; Feng, Y.F. In Vitro Corrosion and Cytocompatibility of a Microarc Oxidation Coating and Poly (L-lactic acid) Composite Coating on Mg-1Li-1Ca Alloy for Orthopedic Implants. *ACS Appl. Mater. Interfaces* **2016**, *8*, 10014–10028. [[CrossRef](#)] [[PubMed](#)]
34. Wang, W.H.; Wu, H.L. Local intragranular misorientation accelerates corrosion in biodegradable Mg. *Acta Biomater.* **2020**, *101*, 575–585. [[CrossRef](#)]
35. Lou, J.; Sun, Y.; Chen, Y.; Zan, R.; Peng, H.; Yang, S.; Kang, X.; Peng, Z.; Wang, W.; Zhang, X. Effects of MgF₂ coating on the biodegradation and biological properties of magnesium. *Surf. Coat. Technol.* **2021**, *422*, 127552. [[CrossRef](#)]

36. Zuo, M.C.; Wang, W.H. In vitro degradation and mineralization of high-purity magnesium in three physiological fluids. *Mater. Lett.* **2019**, *240*, 279–283. [[CrossRef](#)]
37. Williams, G. The Influence of Chloride Ion Concentration on Passivity Breakdown in Magnesium. *Corrosion* **2017**, *73*, 471–481. [[CrossRef](#)]

Disclaimer/Publisher’s Note: The statements, opinions and data contained in all publications are solely those of the individual author(s) and contributor(s) and not of MDPI and/or the editor(s). MDPI and/or the editor(s) disclaim responsibility for any injury to people or property resulting from any ideas, methods, instructions or products referred to in the content.